Normal-state spin dynamics in the iron-pnictide superconductors $BaFe_2(As_{1-x}P_x)_2$ and $Ba(Fe_{1-x}Co_x)_2As_2$ probed with NMR measurements

Y. Nakai,[1,*] T. Iye,[2,3] S. Kitagawa,[2,3] K. Ishida,[2,3,†] S. Kasahara,[2,4] T. Shibauchi,[2] Y. Matsuda,[2] H. Ikeda,[2] and T. Terashima[4]

[1]*Department of Physics, Graduate School of Science and Engineering, Tokyo Metropolitan University, Tokyo 192-0397, Japan*

[2]*Department of Physics, Graduate School of Science, Kyoto University, Kyoto 606-8502, Japan*

[3]*TRIP, JST, Sanban-cho, Chiyoda, Tokyo 102-0075, Japan*

[4]*Research Center for Low Temperature and Materials Sciences, Kyoto University, Kyoto 606-8502, Japan*

(Received 6 March 2013; revised manuscript received 30 April 2013; published 10 May 2013)

The NMR results in iron pnictides $BaFe_2(As_{1-x}P_x)_2$ and $Ba(Fe_{1-x}Co_x)_2As_2$ are analyzed based on the self-consistent renormalization (SCR) spin-fluctuation theory. The temperature dependence of the NMR relaxation rate T_1^{-1} as well as the electrical resistivity is well reproduced by a SCR model where two-dimensional antiferromagnetic (AF) spin fluctuations are dominant. The successful description of the crossover feature from non-Fermi-liquid to Fermi-liquid behavior strongly suggests that low-lying spin fluctuations in $BaFe_2(As_{1-x}P_x)_2$ and $Ba(Fe_{1-x}Co_x)_2As_2$ possess an itinerant AF nature, and that chemical substitution in the two compounds tunes the distance of these systems to an AF quantum critical point. The close relationship between spin fluctuations and superconductivity is discussed compared with the other unconventional superconductors, cuprate and heavy fermion superconductors. In addition, it is suggested that magnetism and lattice instability in these pnictides are strongly linked via orbital degrees of freedom.

DOI: 10.1103/PhysRevB.87.174507 PACS number(s): 76.60.−k, 74.25.nj, 74.40.Kb, 74.70.Xa

I. INTRODUCTION

Since the discovery of high-temperature superconductivity in iron-pnictide superconductors, much effort has been paid to the understanding of the normal and superconducting (SC) state properties, and considerable interest has been focused on the origin of the pairing interaction.[1–3] The proximity of a SC to an antiferromagnetic (AF) phase strongly suggests the interplay between the two ground states. There is accumulating evidence that AF quantum criticality is deeply related to the physics of iron-pnictide superconductors.[4–11] We have studied the spin fluctuations in $BaFe_2(As_{1-x}P_x)_2$ with NMR measurements, and showed that AF spin fluctuations strongly correlate with superconductivity in this system,[7,12] where a line-nodal SC gap structure is suggested.[12–15] These NMR measurements, as well as de Haas–van Alphen (dHvA) experiments, suggest that AF spin fluctuations with a quantum critical nature could be responsible for the "glue" that binds the SC Cooper pairs. In addition, "quantum critical" behavior was reported in a SC parameter, London penetration depth λ_L, which is direct experimental evidence that the superconductivity in $BaFe_2(As_{1-x}P_x)_2$ is linked with its magnetic properties.[16]

In this paper, we analyze in more detail experimental results, particularly the NMR relaxation rate of $BaFe_2(As_{1-x}P_x)_2$ and $Ba(Fe_{1-x}Co_x)_2As_2$. They both possess the "122" structure ($ThCr_2Si_2$ structure) and the recent thermal expansion experiment showed their thermodynamic similarity.[17] These compounds are suggested to be close to an AF quantum critical point (QCP),[6,7] on the basis of the self-consistent renormalization (SCR) theory of spin fluctuations. The SCR theory, developed by Moriya and co-workers, has been applied for weak ferromagnetism and antiferromagnetism of *d*-electron itinerant magnets, and succeeded in characterizing properties of spin fluctuations. As recent studies have shown the importance of both the itinerant and localized nature of the magnetism of iron pnictides,[18–21] it is important to show to what extent experimental results are understood within an itinerant and local-moment picture. Recently, x-ray emission spectroscopy, which is sensitive to very rapid time scales, allowed for the detection of large local moments in the paramagnetic states in iron pnictides.[19,20] In contrast, NMR is a very useful probe to detect much slower fluctuations or low-energy spin excitation, enabling us to extract the itinerant aspects of iron pnictides.

We derive spin-fluctuation parameters in the two compounds by taking into account other experimental results such as the static magnetic susceptibility and specific heat. We calculate the temperature dependences of the NMR relaxation rate and the electrical resistivity following the SCR theory, and show that our calculations are quantitatively consistent with the experimental data. Our analysis indicates that the T_c maximum concentration corresponds to an AF QCP and suggests the possibility of magnetically mediated high-T_c superconductivity in the "122" iron-pnictide superconductors as in other unconventional superconductors of strongly correlated-electron systems.

II. SURVEY OF NMR EXPERIMENTS

Most of our NMR experimental results in $BaFe_2(As_{1-x}P_x)_2$ were published.[7–9] In order to reanalyze our published NMR data in terms of the SCR theory, we summarize them in Figs. 1 and 2.

Figure 1 demonstrates the temperature and P-concentration dependence of the Knight shift in $BaFe_2(As_{1-x}P_x)_2$, which is a measure of the static spin susceptibility $\chi(\boldsymbol{q} = 0)$. The Knight shift is basically T independent, but P substitution reduces the magnitude of the Knight shift. These results are attributable to the decrease in the density of states (DOS) at the Fermi level with P substitution.[22]

Figure 2 displays the temperature dependence of $(T_1T)^{-1}$ for $BaFe_2(As_{1-x}P_x)_2$ with various P concentrations, where P substitution suppresses antiferromagnetism and induces

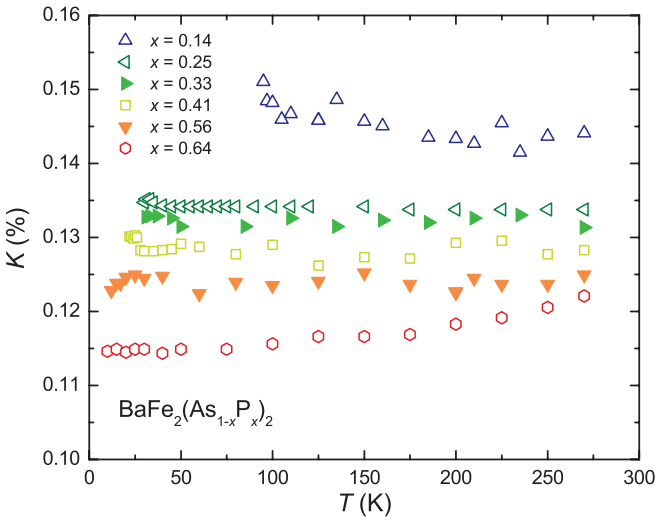

FIG. 1. (Color online) The Knight shift of the ^{31}P nucleus for different P concentrations of $BaFe_2(As_{1-x}P_x)_2$.

superconductivity. We observe non-Fermi-liquid (NFL) temperature dependence of the Curie-Weiss (CW) form $(T_1T)^{-1} = a + b/(T + \theta)$ in the paramagnetic temperature range. For $x \leqslant 0.20$, $(T_1T)^{-1}$ increases on cooling and has a peak at T_N due to the opening of the spin density wave gap, but for $x \geqslant 0.33$, $(T_1T)^{-1}$ exhibits a peak due to a SC gap opening. The CW-type temperature dependence indicates the presence of two-dimensional (2D) AF spin fluctuations according to the SCR theory. The crossover from Fermi-liquid to CW behavior in $(T_1T)^{-1}$ correlates perfectly with the change in the resistivity results.[5] As the system evolves from a Fermi liquid ($x = 0.71$) towards the maximum T_c ($x = 0.33$) near the AF phase, the temperature dependence of the resistivity changes from T^2 to T linear, one hallmark of NFL behavior.

We show in the next section that the CW behavior of $(T_1T)^{-1}$ is consistent with the observed temperature dependences of the electrical resistivity ρ and with the predictions of a SCR model with spin-fluctuation parameters relevant to $BaFe_2(As_{1-x}P_x)_2$.

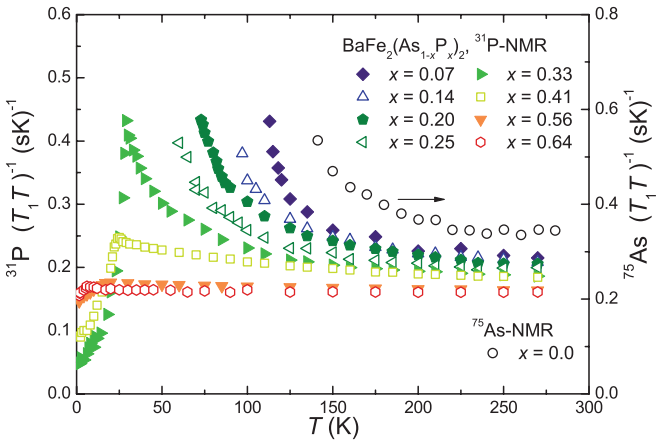

FIG. 2. (Color online) The ^{31}P nuclear spin-lattice relaxation rate divided by temperature $(T_1T)^{-1}$ for $BaFe_2(As_{1-x}P_x)_2$. The data for $x = 0$ ($BaFe_2As_2$) were cited from Ref. 21.

III. ANALYSIS BASED ON THEORY OF SPIN FLUCTUATIONS

In this section, we demonstrate that experimental data of $BaFe_2(As_{1-x}P_x)_2$ and $Ba(Fe_{1-x}Co_x)_2As_2$ are *quantitatively* explainable in terms of the SCR theory for two-dimensional itinerant antiferromagnets. All the NMR data of $Ba(Fe_{1-x}Co_x)_2As_2$ are cited from Ref. 6.

A. Outline of the self-consistent renormalization (SCR) theory

The SCR theory gives quantitative relations between dynamical susceptibility and physical properties. In nearly and weakly AF metals, dynamical susceptibility above T_N for a wave vector near the AF ordering vector $\boldsymbol{Q}$ may generally be written as follows:

$$\chi(\boldsymbol{Q}+\boldsymbol{q},\omega) = \frac{\chi(\boldsymbol{Q}+\boldsymbol{q})}{1 - i\omega/\Gamma_{\boldsymbol{Q}+\boldsymbol{q}}},$$

with

$$[\chi(\boldsymbol{Q}+\boldsymbol{q})]^{-1} = [\chi(\boldsymbol{Q})]^{-1} + Aq^2,$$
$$\Gamma_{\boldsymbol{Q}+\boldsymbol{q}} = \Gamma(\kappa^2 + q^2), \quad \kappa^2 = 1/A\chi(\boldsymbol{Q}),$$

where κ^{-1} ($\equiv\xi_T$) is the temperature-dependent magnetic correlation length, and A and Γ are temperature-independent constants, which are the fundamental parameters of the theory. Using the above relations, the dynamical spin susceptibility $\chi''(\boldsymbol{Q},\omega)$ is written as

$$\chi''(\boldsymbol{Q}+\boldsymbol{q},\omega) = \chi(\boldsymbol{Q}+\boldsymbol{q})\frac{\omega\Gamma_{\boldsymbol{Q}+\boldsymbol{q}}}{\omega^2 + \Gamma^2_{\boldsymbol{Q}+\boldsymbol{q}}} \tag{1}$$

$$= \frac{\chi(Q)\kappa^2}{\kappa^2 + q^2}\frac{\omega\Gamma(\kappa^2+q^2)}{\omega^2 + [\Gamma(\kappa^2+q^2)]^2} \tag{2}$$

$$= \frac{\Gamma}{A}\frac{\omega}{\omega^2 + [\Gamma(\kappa^2+q^2)]^2} \tag{3}$$

$$= \frac{\left(\pi\frac{\Gamma q_B^2}{2\pi}\right)}{\frac{Aq_B^2}{2}}\frac{\omega}{\omega^2 + \left[2\pi\frac{\Gamma q_B^2}{2\pi}\left(\frac{\kappa^2}{q_B^2} + \frac{q^2}{q_B^2}\right)\right]^2} \tag{4}$$

$$= \frac{\pi T_0}{T_A}\frac{\omega}{\omega^2 + \{2\pi T_0[y + (q/q_B)^2]\}^2}, \tag{5}$$

where q_B is the cutoff wave vector and has a relation of $s_0q_B^2/4\pi = 1$ with s_0 being the area per magnetic atom in the 2D plane. In this formula, important spin-fluctuation parameters are the following two characteristic temperatures,

$$T_0 = \Gamma q_B^2/2\pi, \quad T_A = Aq_B^2/2,$$

which characterize the width of the spin excitation spectrum in frequency ω and momentum $\boldsymbol{q}$ space. The dimensionless inverse susceptibility $y(T)$ at $\boldsymbol{Q} = \boldsymbol{Q}_{AF}$ of AF wave vectors is defined as

$$y(T) = \frac{\kappa^2}{q_B^2} = \frac{1}{A\chi(\boldsymbol{Q})q_B^2} = \frac{1}{2T_A\chi(\boldsymbol{Q})}. \tag{6}$$

Here, y_0 is the zero temperature limit of y, and characterizes the proximity to the magnetic instability. $y_0 = 0$ indicates an AF QCP, where $\chi(\boldsymbol{Q})$ diverges down to zero temperature.

The staggered susceptibility or y is determined self-consistently from the relation of the mean square local

amplitude of the zero point and thermal spin fluctuations, and is calculated from

$$y = y_0 + \frac{y_1 t}{2}\{\phi(y/t) - \phi(y/t + 1/t)\}, \tag{7}$$

where $t = T/T_0$, y_1 is the parameter which governs the mode-mode coupling of AF spin fluctuations, and $\phi(x)$ is given as

$$\phi(x) = -\left(x - \frac{1}{2}\right)\log x + x + \log\Gamma(x) - \log\sqrt{2\pi}. \tag{8}$$

B. Calculations of the nuclear spin-lattice relaxation rate T_1^{-1}

The nuclear spin-lattice relaxation rate $1/T_1$ is generally expressed by

$$\frac{1}{T_1} = \frac{\gamma_N^2 T}{N_A}\lim_{\omega\to 0}\sum_{\boldsymbol{q}}\frac{|A_q|^2\chi''(\boldsymbol{q},\omega_0)}{\omega_0}, \tag{9}$$

where γ_N is the gyromagnetic ratio of an observed nucleus, N_A is the number of magnetic atoms per unit volume, A_q is the coupling constant for the hyperfine interaction between the nuclear spin and the q component of the spin density, and ω_0 is the NMR frequency (order of millikelvin). Inserting Eq. (5) into Eq. (9) and neglecting the q dependence of A_q, T_1^{-1} is described as follows:[23]

$$T_1^{-1} = \frac{2\gamma_N^2 A_{\rm hf}^2 T}{N_A}\sum_q \frac{\pi T_0}{T_A\{2\pi T_0[y + (q/q_B)^2]\}^2} \tag{10}$$

$$= \frac{\gamma_N^2 A_{\rm hf}^2}{2\pi T_A}\bar{T}_1^{-1}, \tag{11}$$

$$\bar{T}_1^{-1} = 2\frac{T}{T_0}\int_0^1 dx\,\frac{x}{(y + x^2)^2} = t\left(\frac{1}{y} - \frac{1}{y+1}\right), \tag{12}$$

where $A_{\rm hf}$ is the hyperfine coupling constant. Thus, $1/T_1$ directly measures the temperature dependence of $\chi(\boldsymbol{Q}) = [2T_A y(T)]^{-1}$.

C. Calculations of the electrical resistivity

In the framework of the SCR theory, a predominant contribution to the resistivity arises from the spin fluctuations with AF wave vectors around $\boldsymbol{Q}_{\rm AF}$. The electrical resistivity in a electron system scattered by those spin fluctuations is calculated based on the Boltzmann equation and is given by[23]

$$R(T) = r\bar{R}(T), \tag{13}$$

$$\bar{R}(T) = t\left[\phi\left(\frac{y}{t}\right) - \phi\left(\frac{(y+1)}{t}\right)\right] + y\left[\log\left(\frac{y}{t}\right) - \psi\left(\frac{y}{t}\right)\right] - (y+1)\left[\log\left(\frac{(y+1)}{t}\right) - \psi\left(\frac{(y+1)}{t}\right)\right], \tag{14}$$

where r is an adjustable fitting constant which represents the coupling between the spin fluctuations and conduction electrons, and $\psi(x)$ is the digamma function.

The linear temperature dependence of the resistivity is generic to a QCP of 2D AF metals.[23] Away from the QCP the electrical resistivity shows a crossover from the anomalous T-linear dependence to the Fermi-liquid-like T^2 behavior.

D. Analysis on spin fluctuations in $Ba(Fe_{1-x}Co_x)_2As_2$

Inelastic neutron scattering measurements revealed that two-dimensional spin fluctuations possess stripe correlations [$\boldsymbol{Q}_{\rm AF} = (0,\pi)$ or $(\pi,0)$ in an unfolded Brillouin zone].[24] The presence of the stripe correlations is also suggested from the anisotropy of NMR $1/T_1$ at the As site.[25,26] The T_1 anisotropic ratio $R \equiv {}^{75}(1/T_1T)_{H\perp c}/{}^{75}(1/T_1T)_{H\parallel c} \sim 1.5$ above T_N in $BaFe_2As_2$, $SrFe_2As_2$, and LaFeAsO is consistently understood from the anisotropic spin fluctuations due to the off-diagonal components ($B_{\rm ac}$) of hyperfine coupling tensor $\boldsymbol{B}$ at the As site and from the stripe correlations of the Fe spins.[25–27] The importance of the off-diagonal terms was first pointed out by Kitagawa *et al.*[27]; the internal magnetic fields produced by diagonal terms ($B_{\alpha\alpha}$) are canceled out even if the spin correlations are stripes, since As atoms are located at the symmetrical site with respect to the four nearest-neighbor Fe atoms. The off-diagonal terms related with the stripe correlations are discussed later.

Equations (11) and (12) only give the contribution of spin fluctuations around the AF wave vector $\boldsymbol{Q}_{\rm AF}$. Although the AF contribution around $\boldsymbol{Q}_{\rm AF}$ is expected to be predominant for the NMR relaxation rate in $BaFe_2(As_{1-x}P_x)_2$ and $Ba(Fe_{1-x}Co_x)_2As_2$, there is an additional contribution arising from spin fluctuations around $\boldsymbol{q} = 0$. The observed spin-lattice relaxation rate is thus decomposed into the following two components;

$$\left(\frac{1}{T_1T}\right)_{\rm obs.} = \left(\frac{1}{T_1T}\right)_{\boldsymbol{q}\sim 0} + \left(\frac{1}{T_1T}\right)_{\boldsymbol{q}\sim\boldsymbol{Q}_{\rm AF}}. \tag{15}$$

The experimental NMR results of $Ba(Fe_{1-x}Co_x)_2As_2$ reported by Ning *et al.*[6] show significant AF fluctuations near the optimal doping of $x \sim 0.06$, and that the AF spin fluctuations are systematically suppressed by Co doping. In addition, they reported that $(T_1T)^{-1}$ decreases on cooling for overdoped samples, as observed in LaFeAs(O,F),[26,28,29] indicating that AF spin stripe correlations are not significant in highly overdoped samples. These results are in good agreement with the inelastic neutron scattering measurements.[30] Since the NMR results of $Ba(Fe_{1-x}Co_x)_2As_2$ indicate that the background term of $(T_1T)^{-1}$, which is ascribable to $(T_1T)^{-1}_{\boldsymbol{q}\sim 0}$, shows nonmonotonic behavior, the analysis of contributions from AF fluctuations is less straightforward than $BaFe_2(As_{1-x}P_x)_2$, which will be shown below. By assuming the temperature dependence of the background term of $(T_1T)^{-1}$ is identical with that of the Knight shift, Ning *et al.* estimated the AF contribution and found that its temperature dependence follows a Curie-Weiss-type $(T_1T)^{-1}_{\boldsymbol{q}\sim\boldsymbol{Q}_{\rm AF}} = C/(T+\theta)$ as observed in $BaFe_2(As_{1-x}P_x)_2$.[31] They thus employed the following phenomenological two-component model:

$$(T_1T)^{-1}_{\rm obs.} = (T_1T)^{-1}_{\boldsymbol{q}\sim\boldsymbol{Q}_{\rm AF}} + (T_1T)^{-1}_{\boldsymbol{q}\sim 0}, \tag{16}$$

$$(T_1T)^{-1}_{\boldsymbol{q}\sim 0} = \alpha K_{\rm spin} = \alpha[a + b\exp(-\Delta/k_BT)]. \tag{17}$$

By using their estimation of $(T_1T)^{-1}_{\boldsymbol{q}\sim 0}$,[6,31] the doping dependence of $(T_1)^{-1}_{\boldsymbol{q}\sim\boldsymbol{Q}_{\rm AF}}$ was obtained as shown in Fig. 3. Since $(T_1)^{-1} = $ const behavior is an indication of the verge of a 2D AF QCP (see the next section), we expect a critical Co concentration of $0.05 < x < 0.08$ in $Ba(Fe_{1-x}Co_x)_2As_2$.

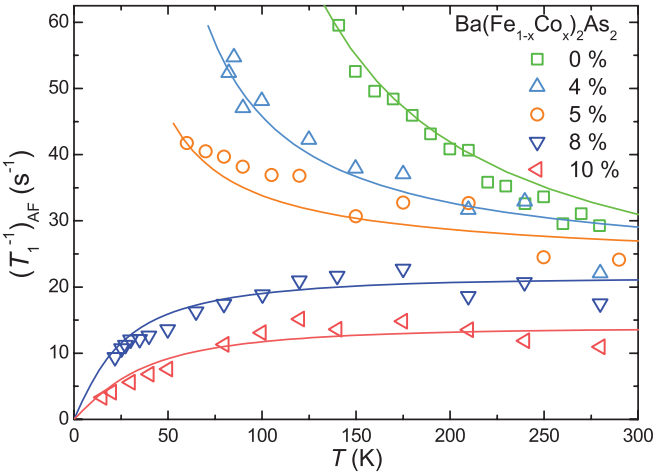

FIG. 3. (Color online) The T dependence of the NMR relaxation rate arising from the $\mathbf{q} \sim \mathbf{Q}_{\rm AF}$ mode of spin fluctuations $(T_1)^{-1}_{\rm AF}$ of $Ba(Fe_{1-x}Co_x)_2As_2$ for $H \parallel ab$, cited from Ref. 6. The solid lines represent simulations with the SCR parameters listed in Table I.

For simulating the NMR data, we need to determine y_0, y_1, T_0, and T_A. In order to narrow down the SCR parameters, we analyzed inelastic neutron scattering data.[30,32] Inosov *et al.* reported that the temperature dependence of the damping constant $\Gamma(T)$ of the dynamical spin susceptibility for nearly optimally doped $Ba(Fe_{0.925}Co_{0.075})_2As_2$ ($T_c = 25$ K) shows a linear temperature dependence $\Gamma(T) = 0.14(T + 30)$(meV). The $\Gamma(T)$ can be calculated in the SCR theory as follows:[33,34]

$$\Gamma(T) = 2\pi T_0 y(T). \tag{18}$$

The T dependence of the Γ is thus sensitive to the parameters of y_0, y_1, and T_0. In this way, we simulate the NMR relaxation rate and neutron scattering data of $x = 0.08$ as shown in Figs. 3 and 4, indicating very good agreement with the experiments.

In order to determine the SCR parameters of other Co doping, we used the data of magnetic susceptibility and specific heat as follows. In the framework of the SCR theory, we can relate the magnetic susceptibility to T_A using the following relation:[33]

$$T_A = 0.75/\chi \quad (\text{in emu/mol}). \tag{19}$$

The estimated T_A of $x = 0.08$ from the NMR and neutron scattering data corresponds to the susceptibility at $T \simeq 200$ K.[35] For other x values, we thus use the T_A values estimated from the susceptibility at 200 K for our calculation.[35] The doping dependence of T_0 is estimated from the reported specific heat experiment[36] by using the following relation:[33,37]

$$\gamma = \frac{6200}{T_0}\left(2x_c - \pi y_0^{-1/2}\right) \quad (\text{mJ/mol K}^2), \tag{20}$$

where x_c is the cutoff wave vector of which magnitude is the order of unity. Note that we used the first term for $y_0 < 0$.[33]

In this way, we simulate the Co concentration dependence of the NMR relaxation rate as shown in Fig. 3 with the SCR parameters as listed in Table I, indicating very good agreement with the experimental data. Using the same parameter, we also calculated the temperature dependence of the electrical resistivity and found good agreement with the experimental result as shown in Fig. 5.

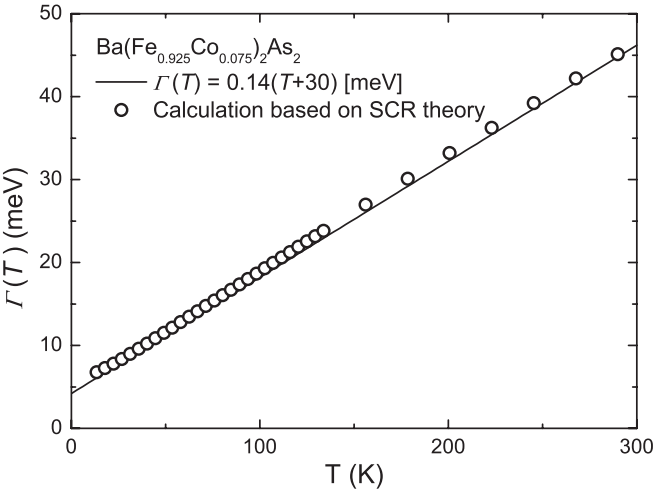

FIG. 4. The experimental (Ref. 32) (solid line) and calculated (circles) damping constant $\Gamma(T)$ for the dynamical susceptibility $\chi''(Q,\omega) = \frac{\chi_T \Gamma(T)\omega}{\omega^2 + \Gamma^2(T)(1+\xi_T^2|Q-Q_{\rm AFM}|)}$ observed in $Ba(Fe_{0.925}Co_{0.075})_2As_2$. The circles represent a calculation with $y_0 = 0.025$, $y_1 = 2.5$, and $T_0 = 450$ K.

TABLE I. The SCR parameters of $Ba(Fe_{1-x}Co_x)_2As_2$.

	y_0	y_1	T_0 (K)	T_A (K)
$x = 0.0$	− 0.4	8.0	460	800
0.04	− 0.07	3.0	510	950
0.05	− 0.03	2.7	530	960
0.08	0.025	2.5	450	1050
0.1	0.05	4.0	420	1200

E. Analysis on spin fluctuations in $BaFe_2(As_{1-x}P_x)_2$

Following a similar procedure as in $Ba(Fe_{1-x}Co_x)_2As_2$, we here analyze the experimental NMR results of $BaFe_2(As_{1-x}P_x)_2$. Because the uniform susceptibility of

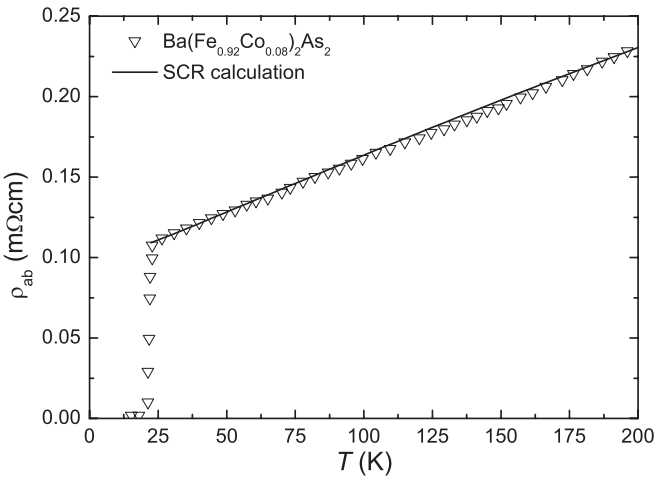

FIG. 5. The T dependence of the electrical resistivity ρ_{ab} of $Ba(Fe_{0.92}Co_{0.08})_2As_2$, cited from Ref. 27. The solid line represents a calculation using $y_0 = 0.025$, $y_1 = 2.5$, and $T_0 = 450$ K, and residual resistivity $\rho_0^{ab} = 0.1$ mΩ cm.

$BaFe_2(As_{1-x}P_x)_2$ is almost temperature independent, the NMR relaxation rate arising from the small-$\boldsymbol{q}$ fluctuations $(T_1T)^{-1}_{\boldsymbol{q}\sim 0}$ is also expected to be temperature independent. In order to estimate $(T_1T)^{-1}_{\boldsymbol{q}\sim 0}$, the observed $(T_1T)^{-1}$ is fit by the CW-type equation $(T_1T)^{-1} = a + b/(T+\theta)$. We relate the first constant term a with the $(T_1T)^{-1}_{\boldsymbol{q}\sim 0}$ and estimated $(T_1)^{-1}_{\boldsymbol{q}\sim \boldsymbol{Q}_{\rm AF}}$ as shown in Fig. 7. The nearly constant $(T_1)^{-1}_{\boldsymbol{q}\sim \boldsymbol{Q}_{\rm AF}}$ of $x = 0.33$ suggests that y_0 is very close to zero at $x = 0.33$.[23]

For simulations of T_1^{-1}, one needs the hyperfine coupling constant $A_{\rm hf}$ of the ^{31}P nucleus. In order to estimate it, it is reasonably assumed that the T_1^{-1} of ^{31}P is determined by the off-diagonal terms of the hyperfine coupling tensor, as is the case for the T_1^{-1} of ^{75}As in $BaFe_2As_2$.[27] Figure 6 displays the T_1^{-1} of ^{75}As for $x = 0.33$ plotted against that of ^{31}P with temperature as an implicit parameter. Since the T_1^{-1} of ^{31}P is proportional to that of ^{75}As as shown in Fig. 6, we can estimate $^{31}A^{\rm off}_{\rm hf} = 6.37$ kOe/μ_B [$\equiv 4(^{31}B_{\rm ac})$] for the ^{31}P nucleus by using $^{75}A^{\rm off}_{\rm hf} = 17.2$ kOe/μ_B [$\equiv 4(^{75}B_{\rm ac})$] for the ^{75}As nucleus.[27] We also assume in our calculations that the hyperfine coupling constant is independent of P concentration.

Although a complete P concentration dependence of magnetic susceptibility and specific heat is not reported in $BaFe_2(As_{1-x}P_x)_2$, we estimate T_0 and T_A as follows. The characteristic spin-fluctuation energy T_0 of $x = 0.33$ with $y_0 = 0$ can be estimated from reported specific heat experiments[14] by using Eq. (20). Assuming that the P concentration dependence of γ is identical with that of $K_{\rm spin}$, which is the measure of the DOS at the Fermi energy,[7] we can estimate γ for other P concentrations and obtain the P concentration dependence of T_0 using Eq. (20). We here neglect the second term in Eq. (20) for simplicity. In order to estimate T_A from Eq. (19), we assume the magnetic susceptibility χ is proportional to $K_{\rm spin}$. By using $\chi = 9.4\times 10^{-4}$ emu/mol at 200 K and $\gamma = 27$ mJ/mol K^2 in $BaFe_2As_2$,[35,36] we thus estimate the P concentration dependence of T_A.

By using the SCR parameters listed in Table II, which are obtained from our NMR simulation shown in Fig. 7, we calculated the temperature exponent of electrical resistivity. For 2D AF fluctuations, a T-linear resistivity is expected near the QCP.[38] Away from the QCP, the temperature dependence of the resistivity crossovers to a Fermi-liquid-like T^2 as T decreases. The experimental data is actually consistent with the simulated temperature dependence as shown in Fig. 8.

According to the SCR theory, we can also estimate the in-plane spin correlation length $\xi(T)$ and the damping constant $\Gamma(T)$ from $(\sqrt{4\pi y})^{-1}$ and from $2\pi T_0 y$, respectively.[39] We calculated ξ/a and $\Gamma(T)$ at T_c for different P concentrations as shown in Table II, which may be confirmed by future neutron scattering experiments.

TABLE II. The SCR parameters of $BaFe_2(As_{1-x}P_x)_2$. The in-plane spin correlation length ξ/a and damping constant Γ at T_c are also shown. Note that a is the in-plane lattice constant.

	y_0	y_1	T_0 (K)	T_A (K)	$\xi(T_c)/a$	$\Gamma(T_c)$ (meV)
$x = 0.0$	-0.4	8.0	460	800		
0.2	-0.15	15	760	1320		
0.25	-0.05	10	770	1340	3.0	3.7
0.33	0	8.0	780	1350	1.9	9.2
0.41	0.06	5.0	800	1390	1.1	27
0.56	0.2	6.0	850	1480	0.6	96

IV. DISCUSSION

A. Phase diagrams

The phase diagrams of $BaFe_2(As_{1-x}P_x)_2$ and $Ba(Fe_{1-x}Co_x)_2As_2$ are plotted in Fig. 9. The y_0 increases with chemical substitution from a negative value in $BaFe_2As_2$ to nearly zero around an optimal concentration: $x \sim 0.3$ for $BaFe_2(As_{1-x}P_x)_2$ and $x \sim 0.06$ for $Ba(Fe_{1-x}Co_x)_2As_2$. Since y_0 is a measure of the closeness to a QCP, this indicates that

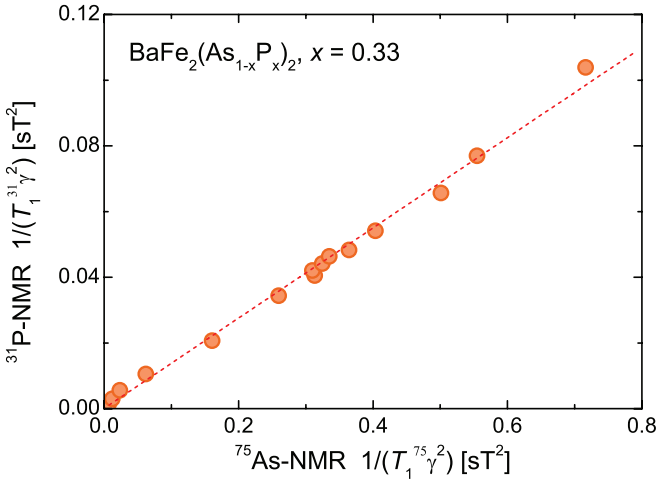

FIG. 6. (Color online) The T_1^{-1} of ^{31}P and ^{75}As in $BaFe_2(As_{1-x}P_x)_2$ with $x = 0.33$ is plotted. We estimated the hyperfine coupling constant of ^{31}P nucleus from the slope as $^{31}A_{\rm hf} = 0.674$ T/μ_B by using $^{75}A_{\rm hf} = 1.72$ T/μ_B (Ref. 27).

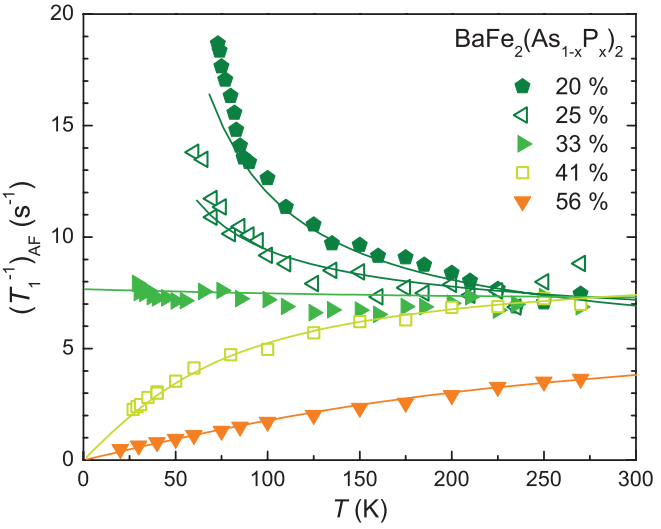

FIG. 7. (Color online) The experimental and calculated NMR relaxation rate arising from the $\boldsymbol{q} \sim \boldsymbol{Q}_{\rm AF}$ mode of spin fluctuations in $BaFe_2(As_{1-x}P_x)_2$. The data points represent the experimental data, while the solid lines indicate the calculated data using the SCR parameters listed in Table II.

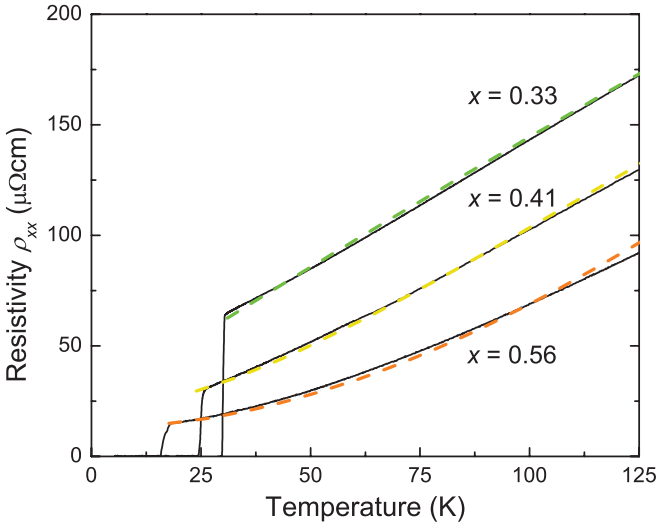

FIG. 8. (Color online) The experimental (Ref. 5) and calculated electrical resistivity of $BaFe_2(As_{1-x}P_x)_2$. The solid lines represent the experimental data, while the dotted lines indicate the calculated data using the SCR parameters listed in Table II.

their optimal concentration corresponds to an AF QCP and the closeness to the QCP is controllable by P and Co substitution.

B. Spin-fluctuation temperature T_0,T_A versus SC transition temperature T_c

In $BaFe_2(As_{1-x}P_x)_2$ and $Ba(Fe_{1-x}Co_x)_2As_2$, the SC phase exists next to the AF phase, and T_c is maximum nearly at an AF QCP, i.e., $y_0 \sim 0$, as shown in Fig. 9. This strongly suggests that there is an intimate link between superconductivity and antiferromagnetism in iron-pnictide superconductors. This is reminiscent of heavy-fermion (HF) superconductors, particularly Ce-based superconductors such as $CeCu_2Si_2$ and $CeMIn_5$ (M: Co, Rh, and Ir).[40] In these Ce-based HF superconductors, superconductivity occurs near an AF QCP, which is induced by competition between the Ruderman-Kittel-Kasuya-Yosida (RKKY) interaction and the Kondo effect. A number of experiments in these HF superconductors reported NFL behavior [e.g., $\rho(T) \propto T^{\alpha}$ over a wide T range at low temperatures] near the QCP. The NFL behavior is ascribed to AF spin fluctuations with a quantum critical nature, and the AF spin fluctuations likely induce unconventional superconductivity with a d-wave order parameter. Similarly, AF fluctuations are also suggested for a likely candidate of the pairing mechanism for high-T_c cuprate superconductors where significant NFL behavior is observed, although understanding of the pseudogap behavior in the normal state has not been settled.

In order to understand a relationship between AF spin fluctuations and superconductivity, we plot SC T_c against spin-fluctuation parameters T_0 and T_A of $BaFe_2(As_{1-x}P_x)_2$ and $Ba(Fe_{1-x}Co_x)_2As_2$ as well as those of unconventional superconductors in Fig. 10. Note that only optimal $BaFe_2(As_{1-x}P_x)_2$ and nearly optimal $Ba(Fe_{1-x}Co_x)_2As_2$ are plotted, since the (nearly) optimal samples are close to an AF QCP.[38,41] The linear scaling between the spin-fluctuation temperature T_0 and T_c in Ce-based HF superconductors and the cuprates was interpreted as an indication of spin-fluctuation mediated

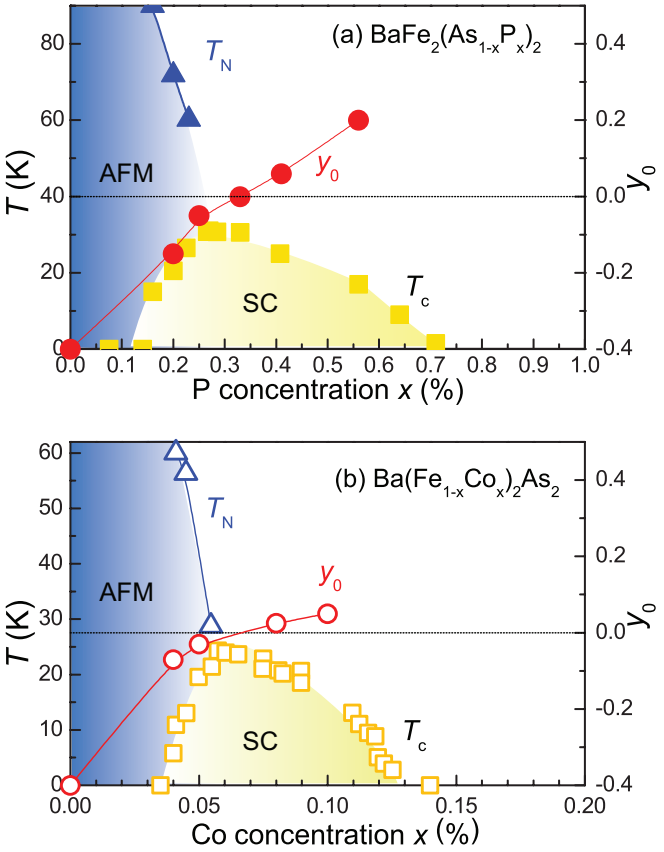

FIG. 9. (Color online) Phase diagrams of $BaFe_2(As_{1-x}P_x)_2$ and $Ba(Fe_{1-x}Co_x)_2As_2$, where T_N and T_c denote an AF transition temperature and SC transition temperature, respectively. In both materials, the concentration where T_c peaks [$x \sim 0.3$ for $BaFe_2(As_{1-x}P_x)_2$, and $x \sim 0.06$ for $Ba(Fe_{1-x}Co_x)_2As_2$] exists near the region where $y_0 = 0$. Since $y_0 = 0$ corresponds to an AF QCP, these phase diagrams suggest a close link between superconductivity and AF quantum criticality.

superconductivity in these unconventional superconductors and that a higher spin-fluctuation temperature can give rise to a pairing interaction and thus resulting in higher T_c.[38,41] Interestingly, optimal $BaFe_2(As_{1-x}P_x)_2$ has a higher T_0 and T_c than $Ba(Fe_{1-x}Co_x)_2As_2$, and these "122" iron-pnictide superconductors have intermediate values of T_0 and T_c among other unconventional superconductors. This suggests that the physics of "122" iron-pnictide superconductors may be more closely related to the physics of HF and cuprate superconductors than previously expected, and they may be classified into magnetically mediated superconductors. Moreover, only the optimal superconductivity lies on the curve. This suggests that quantum criticality is another important ingredient for an understanding of the linearity between spin-fluctuation temperature and T_c, as discussed in the HF superconductors such as $CeMIn_5$.[42,43]

In addition, it is noteworthy that T_A is roughly scaled to T_c as shown in Fig. 10(b), and hence to T_0. This implies that the spin-fluctuation spectra are renormalized with T_0, as indeed inferred from Fig. 11, where the renormalized $(T_1T)^{-1}$ of various unconventional superconductors approximately scales onto a same curve against T/T_c. Because T_c values in these

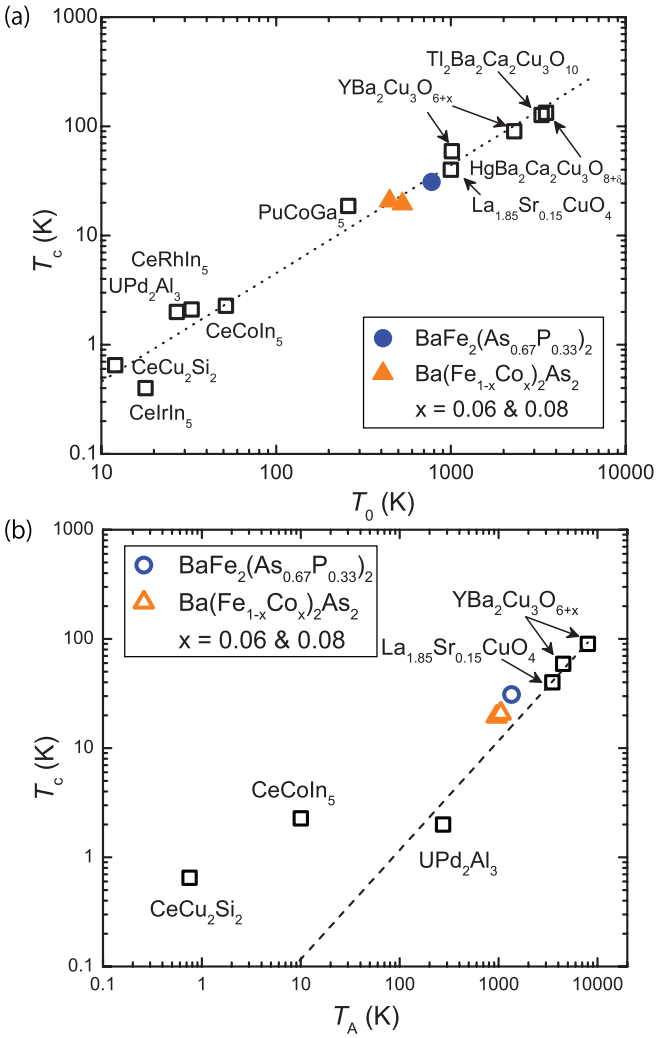

FIG. 10. (Color online) The SC transition temperature T_c vs the spin-fluctuation temperature (a) T_0 and (b) T_A for various superconductors. The data for T_c and T_0 were cited from Refs. 35 and 37. The dotted lines represent linear curve fittings. T_c is linear with T_0, as suggested in Ref. 35, and the iron-pnictide superconductors lie on the same line. This may be the signature that Fe pnictides, heavy-fermion, and cuprate superconductors are mediated by AF spin fluctuations.

superconductors are different by two orders of magnitude, the scaling of $(T_1T)^{-1}$ is surprising and suggests that spin-fluctuation spectra are related with their unconventional superconductivity.

C. Coupling between AF spin fluctuations and lattice instability

In this section, we comment on the relationship between magnetism and lattice structure in the "122" compounds. A structural transition from the high-temperature tetragonal to low-temperature orthorhombic phases occurs at T_S that is identical to T_N or just above T_N. Since the structural unit vectors rotates by 45° at the transition, the dotted lines in Fig. 12 represent the distorted basal plane below T_S, which is a unit cell above T_S. An unusual anisotropic interaction ($J_{1a} > J_{1b}, J_{1a} \sim J_2$) was reported in the ordered state from the neutron scattering experiments.[48] We suggest that the

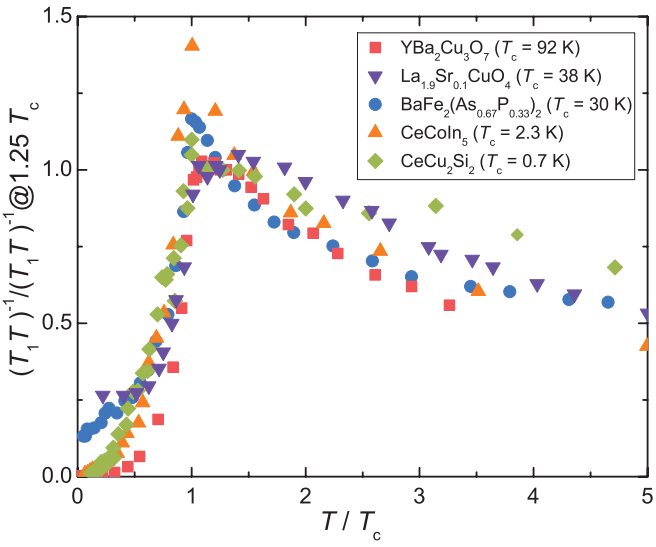

FIG. 11. (Color online) The T dependence of $(T_1T)^{-1}$ normalized by $(T_1T)^{-1}$ at $1.25T_c$ in various unconventional superconductors (Refs. 44–47) are plotted against T/T_c. $(T_1T)^{-1}$ at $1.25T_c$ is adopted in order to avoid the suppression by the pseudogap effect. The characteristic energy of the spin fluctuations in these compounds seems to be scaled to T_c, since the normalized $(T_1T)^{-1}$ data are approximately on the same curve.

anisotropic interactions are reasonably understood by the coupling between four Fe sites by way of the As site as follows. Kitagawa *et al.* reported that the electric quadrupole interaction (ν) at the As site changes significantly below T_S: ν_a along the a axis becomes largest, although the difference between the lattice constant a and b is less than 1%.[27] This strongly suggests that the isotropic charge distribution above T_S becomes anisotropic, resulting in a higher electron occupation in $4p_x$ than that in $4p_y$. A similar conclusion was drawn from angle-resolved photoemission spectroscopy

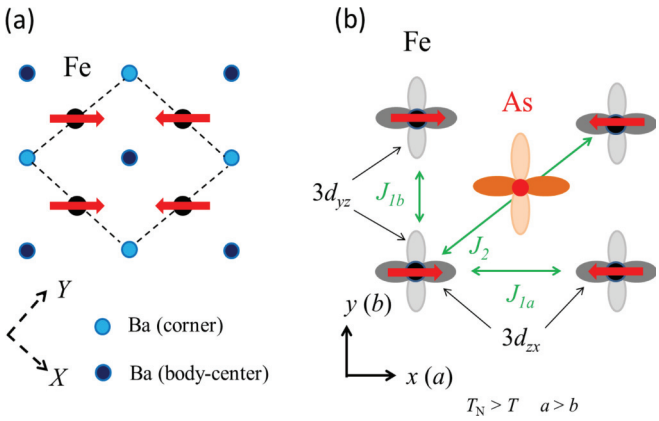

FIG. 12. (Color online) (a) Low-temperature magnetic structure at the Fe layer. The Ba sites are also shown. The dotted lines indicate the tetragonal unit cell above T_S, and are deformed below T_S. The stripe magnetic structure is shown by the arrows. (b) As $4p_{x,y}$ and Fe $3d_{yz}$ and $3d_{zx}$ orbitals are shown. The difference in the electronic population is shown by the contrasting density. Magnetic interactions between the nearest neighbor and next nearest neighbor are denoted by arrows.

(ARPES) experiments.[49] Such an imbalance of occupation implies that degenerate Fe $3d_{xz}$ and $3d_{yz}$ orbitals are lifted due to nonequivalent mixing with As $4p_x$ and $4p_y$ orbitals, in other words, orbital ordering of the Fe $3d$ orbitals is realized. This symmetry breaking naturally leads to a deviation of the exchange interaction J_1 between the nearest-neighbor Fe spins. The corresponding orthorhombic distortion can make a J_{1b} ferromagnetic interaction rather than an antiferromagnetic one, following the Goodenough-Kanamori rules, because the Fe-As-Fe bond angle for J_{1a} becomes close to 90°. Such a tendency is consistent with the recent studies by the neutron scattering measurements.[18]

It is naturally expected that the above anisotropic correlations persist well above T_N, since the stripe AFM fluctuations are observed in the tetragonal phase, and thus the orbital fluctuations linked with the characteristic stripe AF spin correlations are anticipated above T_N. Actually, such lattice dynamics was observed with ultrasonic experiments. Goto *et al.* and Yoshizawa *et al.* reported independently that the elastic constant C_{66} in $Ba(Fe_{1-x}Co_x)_2As_2$ shows a large elastic softening towards T_S.[50,51] The latter group pointed out that the Co concentration dependence of the C_{66} softening is ascribable to the presence of a "structural QCP," similar to a magnetic QCP, and suggested that the high T_c in $Ba(Fe_{1-x}Co_x)_2As_2$ is related to the structural QCP.[50] Since the temperature dependence of C_{66} is quite similar to that of $(T_1T)^{-1}_{AF}$ of AF spin fluctuations, we plot the temperature dependence of C_{66} against that of $(T_1T)^{-1}_{AF}$ with T as an implicit parameter, as shown in Fig. 13. An apparent proportionality between the two quantities strongly suggests that AF spin fluctuations and structural fluctuations are closely related, indicative of sharing the same origin.

Quite recently Kasahara *et al.* reported from the torque magnetometry and precise x-ray measurements that the fourfold symmetry is broken in $BaFe_2(As_{1-x}P_x)_2$ below T^* that is much higher than T_S, and suggested the formation of an electronic nematic state below T^*.[52] We compare temperature and P concentration dependences of T^* and $(T_1T)^{-1}$ in Fig. 14, where the values of $(T_1T)^{-1}$ are shown as a contour plot.

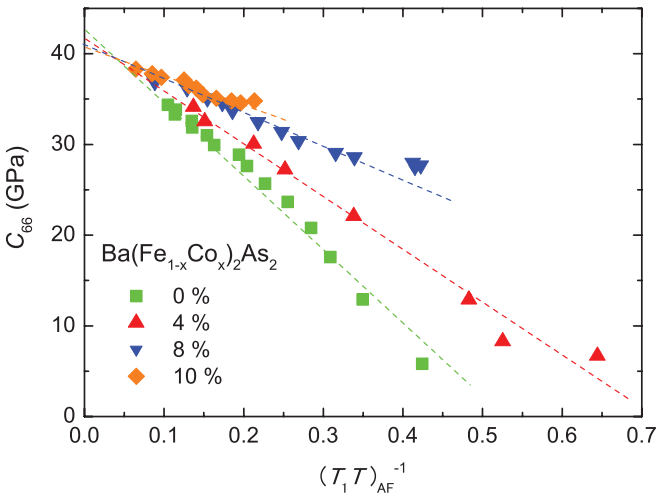

FIG. 13. (Color online) The T dependence of the elastic constant C_{66} in $Ba(Fe_{1-x}Co_x)_2As_2$, measured by Yoshizawa *et al.* (Ref. 50), is plotted against $(T_1T)^{-1}_{AF}$ of Fig. 6. An apparent proportionality holds between C_{66} and $(T_1T)^{-1}_{AF}$. The dotted lines are guides to the eyes.

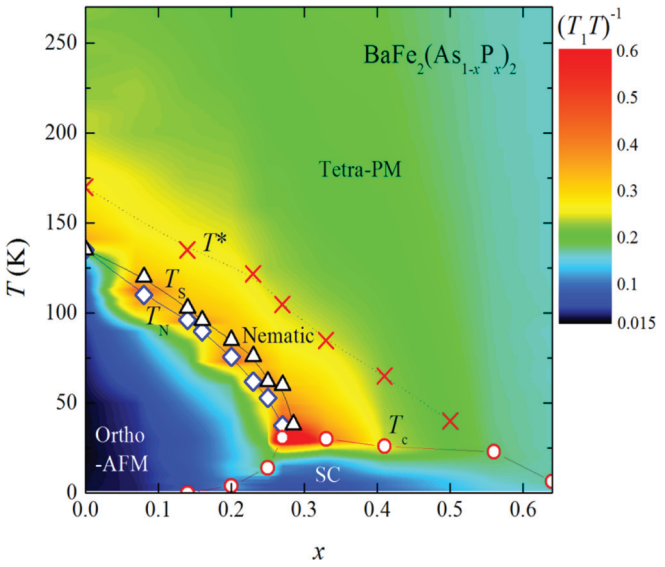

FIG. 14. (Color online) The nematic transition temperature T^* and $(T_1T)^{-1}$ are compared. The magnitude of $(T_1T)^{-1}$ is shown as a contour plot. $(T_1T)^{-1}$ seems to increase below T^*, particularly in the low P concentration, suggestive of a close relationship between T^* and AF spin fluctuations.

It seems that $(T_1T)^{-1}$ starts to be enhanced approximately below T^*, particularly obvious in the low concentration region. The enhancement below T^* can be understood by the fact that the development of the stripe AFM correlations should be determined by breaking the fourfold symmetry in the tetragonal phase, resulting in that the direction of the stripe correlations is fixed and that the correlation length is allowed to be extended more easily.

The iron-pnictide compounds are thus a unique system, where the spin and orbital degrees of freedom are strongly coupled with each other. Although we indicated here that the spin-fluctuation theory is successfully applicable to the 122 systems, the interplay between the spin fluctuation and the orbital degrees of freedom remains to be solved in the future.

V. CONCLUSION

We show that the temperature dependences of the NMR nuclear spin-lattice relaxation rate, the electrical resistivity, and the inelastic neutron scattering data in the paramagnetic phase of iron-pnictide superconductors $BaFe_2(As_{1-x}P_x)_2$ and $Ba(Fe_{1-x}Co_x)_2As_2$ can be understood quantitatively in the framework of the SCR theory. A consistent description of these physical properties of $BaFe_2(As_{1-x}P_x)_2$ and $Ba(Fe_{1-x}Co_x)_2As_2$ in the framework of the SCR theory suggests that an itinerant picture is at work for the "122" iron-pnictide superconductors at the low-energy scale and AF quantum criticality would be deeply related to the high-T_c superconductivity, as in other unconventional superconductors. However, a puzzling question in iron-pnictide superconductors is whether AF spin fluctuations and superconductivity are deeply related in "1111" systems such as $LaFeAs(O_{1-x}F_x)$ and $Ca(Fe_{1-x}Co_x)AsF$.[26,28,53–55] In addition, the phase diagram in these systems is different from that in the Ba-"122" systems. Indeed, it was reported recently that superconductivity in

$LaFeAs(O_{1-x}H_x)$ possesses a two-maximum structure and survives until higher hole concentration.[56] It seems that the superconductivity can be observed in the region away from the AF QCP, indicating that the scenarios of superconductivity induced by AF spin fluctuations may not be applied universally. Whether a unified picture exists for explaining all experimental results in iron-pnictide superconductors, or whether there exist mechanisms other than magnetism, are a future important issue to be clarified.

ACKNOWLEDGMENTS

We are grateful to S. Yonezawa and Y. Maeno for fruitful discussions. This work is supported by Grants-in-Aid for Scientific Research on Innovative Areas "Heavy Electrons" (No. 20102006) from MEXT, for the GCOE Program "The Next Generation of Physics, Spun from Universality and Emergence" from MEXT, and for Scientific Research from JSPS. Y.N. is supported by KAKENHI (No. 23654120).

*nakai@tmu.ac.jp

†kishida@scphys.kyoto-u.ac.jp

[1] Y. Kamihara, T. Watanabe, M. Hirano, and H. Hosono, J. Am. Chem. Soc. **130**, 3296 (2008).

[2] K. Ishida, Y. Nakai, and H. Hosono, J. Phys. Soc. Jpn. **78**, 062001 (2009).

[3] J. Paglione and R. L. Greene, Nat. Phys. **6**, 645 (2010).

[4] S. Jiang, H. Xing, G. Xuan, C. Wang, Z. Ren, C. Feng, J. Dai, Z. Xu, and G. Cao, J. Phys.: Condens. Matter **21**, 382203 (2009).

[5] S. Kasahara, T. Shibauchi, K. Hashimoto, K. Ikada, S. Tonegawa, R. Okazaki, H. Shishido, H. Ikeda, H. Takeya, K. Hirata *et al.*, Phys. Rev. B **81**, 184519 (2010).

[6] F. L. Ning, K. Ahilan, T. Imai, A. S. Sefat, M. A. McGuire, B. C. Sales, D. Mandrus, P. Cheng, B. Shen, and H.-H. Wen, Phys. Rev. Lett. **104**, 037001 (2010).

[7] Y. Nakai, T. Iye, S. Kitagawa, K. Ishida, H. Ikeda, S. Kasahara, H. Shishido, T. Shibauchi, Y. Matsuda, and T. Terashima, Phys. Rev. Lett. **105**, 107003 (2010).

[8] T. Iye, Y. Nakai, S. Kitagawa, K. Ishida, S. Kasahara, T. Shibauchi, Y. Matsuda, and T. Terashima, J. Phys. Soc. Jpn. **81**, 033701 (2012).

[9] T. Iye, Y. Nakai, S. Kitagawa, K. Ishida, S. Kasahara, T. Shibauchi, Y. Matsuda, and T. Terashima, Phys. Rev. B **85**, 184505 (2012).

[10] J. Dai, Q. Si, J.-X. Zhu, and E. Abrahams, Proc. Natl. Acad. Sci. USA **106**, 4118 (2009).

[11] S. Sachdev and B. Keimer, Phys. Today **64**(2), 29 (2011).

[12] Y. Nakai, T. Iye, S. Kitagawa, K. Ishida, S. Kasahara, T. Shibauchi, Y. Matsuda, and T. Terashima, Phys. Rev. B **81**, 020503(R) (2010).

[13] K. Hashimoto, M. Yamashita, S. Kasahara, Y. Senshu, N. Nakata, S. Tonegawa, K. Ikada, A. Serafin, A. Carrington, T. Terashima *et al.*, Phys. Rev. B **81**, 220501 (2010).

[14] J. S. Kim, P. J. Hirschfeld, G. R. Stewart, S. Kasahara, T. Shibauchi, T. Terashima, and Y. Matsuda, Phys. Rev. B **81**, 214507 (2010).

[15] M. Yamashita, Y. Senshu, T. Shibauchi, S. Kasahara, K. Hashimoto, D. Watanabe, H. Ikeda, T. Terashima, I. Vekhter, A. B. Vorontsov *et al.*, Phys. Rev. B **84**, 060507 (2011).

[16] K. Hashimoto, K. Cho, T. Shibauchi, S. Kasahara, Y. Mizukami, R. Katsumata, Y. Tsuruhara, T. Terashima, H. Ikeda, M. A. Tanatar *et al.*, Science **336**, 1554 (2012).

[17] A. E. Böhmer, P. Burger, F. Hardy, T. Wolf, P. Schweiss, R. Fromknecht, H. v. Löhneysen, C. Meingast, H. K. Mak, R. Lortz *et al.*, Phys. Rev. B **86**, 094521 (2012).

[18] P. Dai, J. Hu, and E. Dagotto, Nat. Phys. **8**, 709 (2012).

[19] H. Gretarsson, A. Lupascu, J. Kim, D. Casa, T. Gog, W. Wu, S. R. Julian, Z. J. Xu, J. S. Wen, G. D. Gu *et al.*, Phys. Rev. B **84**, 100509 (2011).

[20] P. Vilmercati, A. Fedorov, F. Bondino, F. Offi, G. Panaccione, P. Lacovig, L. Simonelli, M. A. McGuire, A. S. M. Sefat, D. Mandrus *et al.*, Phys. Rev. B **85**, 220503 (2012).

[21] L. P. Gor'kov and G. B. Teitel'baum, Phys. Rev. B **87**, 024504 (2013).

[22] H. Ikeda, J. Phys. Soc. Jpn. **77**, 123707 (2008).

[23] T. Moriya, Y. Takahashi, and K. Ueda, J. Phys. Soc. Jpn. **59**, 2905 (1990).

[24] M. Ishikado, Y. Nagai, K. Kodama, R. Kajimoto, M. Nakamura, Y. Inamura, S. Wakimoto, H. Nakamura, M. Machida, K. Suzuki *et al.*, Phys. Rev. B **84**, 144517 (2011).

[25] K. Kitagawa, N. Katayama, K. Ohgushi, and M. Takigawa, J. Phys. Soc. Jpn. **78**, 063706 (2009).

[26] S. Kitagawa, Y. Nakai, T. Iye, K. Ishida, Y. Kamihara, M. Hirano, and H. Hosono, Phys. Rev. B **81**, 212502 (2010).

[27] K. Kitagawa, N. Katayama, K. Ohgushi, M. Yoshida, and M. Takigawa, J. Phys. Soc. Jpn. **77**, 114709 (2008).

[28] Y. Nakai, K. Ishida, Y. Kamihara, M. Hirano, and H. Hosono, J. Phys. Soc. Jpn. **77**, 073701 (2008).

[29] Y. Nakai, S. Kitagawa, K. Ishida, Y. Kamihara, M. Hirano, and H. Hosono, New J. Phys. **11**, 045004 (2009).

[30] K. Matan, S. Ibuka, R. Morinaga, S. Chi, J. W. Lynn, A. D. Christianson, M. D. Lumsden, and T. J. Sato, Phys. Rev. B **82**, 054515 (2010).

[31] K. Ahilan, F. L. Ning, T. Imai, A. Sefat, M. A. McGuire, B. C. Sales, D. Mandrus, P. Cheng, B. Shen, and H. Wen, arXiv:0910.1071.

[32] D. S. Inosov, J. T. Park, P. Bourges, D. L. Sun, Y. Sidis, A. Schneidewind, K. Hradil, D. Haug, C. T. Lin, B. Keimer *et al.*, Nat. Phys. **6**, 178 (2010).

[33] T. Moriya and T. Takimoto, J. Phys. Soc. Jpn. **64**, 960 (1995).

[34] S. Kambe, H. Sakai, Y. Tokunaga, T. D. Matsuda, Y. Haga, H. Chudo, and R. E. Walstedt, Phys. Rev. B **77**, 134418 (2008).

[35] X. F. Wang, T. Wu, G. Wu, R. H. Liu, H. Chen, Y. L. Xie, and X. H. Chen, New J. Phys. **11**, 045003 (2009).

[36] F. Hardy, P. Burger, T. Wolf, R. A. Fisher, P. Schweiss, P. Adelmann, R. Heid, R. Fromknecht, R. Eder, D. Ernst *et al.*, Europhys. Lett. **91**, 47008 (2010).

[37] T. Moriya and K. Ueda, J. Phys. Soc. Jpn. **63**, 1871 (1994).

[38] T. Moriya and K. Ueda, Rep. Prog. Phys. **66**, 1299 (2003).

[39] T. Moriya and K. Ueda, Adv. Phys. **49**, 555 (2000).

[40] C. Pfleiderer, Rev. Mod. Phys. **81**, 1551 (2009).

[41] N. J. Curro, T. Caldwell, E. D. Bauer, L. A. Morales, M. J. Graf, Y. Bang, A. V. Balatsky, J. D. Thompson, and J. L. Sarrao, Nature (London) **434**, 622 (2005).

[42]P. Gegenwart, Q. Si, and F. Steglich, Nat. Phys. **4**, 186 (2008).
[43]T. Park, F. Ronning, H. Q. Yuan, M. B. Salamon, R. Movshovich, J. L. Sarrao, and J. D. Thompson, Nature (London) **440**, 65 (2006).
[44]K. Ishida, Y. Kitaoka, N. Ogata, T. Kamino, K. Asayama, J. R. Cooper, and N. Athanassopoulou, J. Phys. Soc. Jpn. **62**, 2803 (1993).
[45]S. Ohsugi, Y. Kitaoka, K. Ishida, and K. Asayama, J. Phys. Soc. Jpn. **60**, 2351 (1991).
[46]Y. Kawasaki, S. Kawasaki, M. Yashima, T. Mito, G. q. Zheng, Y. Kitaoka, H. Shishido, R. Settai, Y. Haga, and Y. Ōnuki, J. Phys. Soc. Jpn. **72**, 2308 (2003).
[47]K. Ishida, Y. Kawasaki, K. Tabuchi, K. Kashima, Y. Kitaoka, K. Asayama, C. Geibel, and F. Steglich, Phys. Rev. Lett. **82**, 5353 (1999).
[48]D. C. Johnston, Adv. Phys. **59**, 803 (2010).
[49]T. Shimojima, K. Ishizaka, Y. Ishida, N. Katayama, K. Ohgushi, T. Kiss, M. Okawa, T. Togashi, X.-Y. Wang, C.-T. Chen *et al*., Phys. Rev. Lett. **104**, 057002 (2010).
[50]M. Yoshizawa, D. Kimura, T. Chiba, S. Simayi, Y. Nakanishi, K. Kihou, C. H. Lee, A. Iyo, H. Eisaki, M. Nakajima *et al*., J. Phys. Soc. Jpn. **81**, 024604 (2012).
[51]T. Goto, R. Kurihara, K. Araki, K. Mitsumoto, M. Akatsu, Y. Nemoto, S. Tatematsu, and M. Sato, J. Phys. Soc. Jpn. **80**, 073702 (2011).
[52]S. Kasahara, H. J. Shi, K. Hashimoto, S. Tonegawa, Y. Mizukami, T. Shibauchi, K. Sugimoto, T. Fukuda, T. Terashima, A. H. Nevidomskyy *et al*., Nature (London) **486**, 382 (2012).
[53]Y. Kobayashi, E. Satomi, S. C. Lee, and M. Sato, J. Phys. Soc. Jpn. **79**, 093709 (2010).
[54]T. Oka, Z. Li, S. Kawasaki, G. F. Chen, N. L. Wang, and G.-q. Zheng, Phys. Rev. Lett. **108**, 047001 (2012).
[55]S. Tsutsumi, N. Fujiwara, S. Matsuishi, and H. Hosono, Phys. Rev. B **86**, 060515 (2012).
[56]S. Iimura, S. Matuishi, H. Sato, T. Hanna, Y. Muraba, S. W. Kim, J. E. Kim, M. Takata, and H. Hosono, Nat. Commun. **3**, 943 (2012).